Molecular Signature of 18 F-FDG PET Biomarkers in Newly Diagnosed Multiple Myeloma Patients: A Genome-Wide Transcriptome Analysis from the CASSIOPET Study

Jean-Baptiste Alberge, Françoise Kraeber-Bodéré, Bastien Jamet, Cyrille Touzeau, Hélène Caillon, Soraya Wuilleme, Marie-Christine Béné, Tobias Kampfenkel, Pieter Sonneveld, Mark van Duin, et al.

▶ **To cite this version:**

Jean-Baptiste Alberge, Françoise Kraeber-Bodéré, Bastien Jamet, Cyrille Touzeau, Hélène Caillon, et al.. Molecular Signature of 18 F-FDG PET Biomarkers in Newly Diagnosed Multiple Myeloma Patients: A Genome-Wide Transcriptome Analysis from the CASSIOPET Study. Journal of Nuclear Medicine, 2022, 63 (7), pp.1008-1013. 10.2967/jnumed.121.262884 . hal-03807107

HAL Id: hal-03807107
https://hal.science/hal-03807107

Submitted on 11 Oct 2022

HAL is a multi-disciplinary open access archive for the deposit and dissemination of scientific research documents, whether they are published or not. The documents may come from teaching and research institutions in France or abroad, or from public or private research centers.

L'archive ouverte pluridisciplinaire **HAL**, est destinée au dépôt et à la diffusion de documents scientifiques de niveau recherche, publiés ou non, émanant des établissements d'enseignement et de recherche français ou étrangers, des laboratoires publics ou privés.

Molecular signature of FDG-PET biomarkers in newly diagnosed multiple myeloma patients: a genome-wide transcriptome analysis from the CASSIOPET study

Jean-Baptiste Alberge[1,2], Françoise Kraeber-Bodéré[1,2,3,4,5], Bastien Jamet[2,3] Cyrille Touzeau[1,2,5], Hélène Caillon[5], Soraya Wuilleme[5], Marie-Christine Béné[5], Tobias Kampfenkel[6], Pieter Sonneveld[7], Mark van Duin[7], Herve Avet-Loiseau[8], Jill Corre[8], Florence Magrangeas[1,2,5], Thomas Carlier[1,2,3], Caroline Bodet-Milin[1,2,3], Michel Chérel[1,2,4], Philippe Moreau[1,2,5], Stéphane Minvielle[1,2,5], Clément Bailly [1,2,3]

[1] Université de Nantes, CHU Nantes, CNRS, Inserm, CRCINA, F-44000 Nantes, France.

[2] Site de Recherche Intégrée sur le Cancer (SIRIC), Imaging and Longitudinal Investigations to Ameliorate Decision-making (ILIAD), INCA-DGOS-Inserm 12558, Nantes, France

[3] Nuclear Medicine Unit, University Hospital, 44093 Nantes, France.

[4] Nuclear Medicine Unit, ICO-Gauducheau, 44805 Nantes-Saint-Herblain, France.

[5] Haematology Department, University Hospital, 44093 Nantes, France.

[6] Janssen Research & Development, LLC, Leiden.

[7] Erasmus University Medical Center Cancer Institute, Rotterdam, Netherlands

[8] Unité de de Génomique du Myélome, Institut universitaire du cancer de Toulouse Institut National de la Santé, 31300 Oncopole, Toulouse, France

Correspondence to: Clément Bailly Nuclear Medicine Unit, University Hospital, 44093 Nantes, France : clement.bailly@chu-nantes.fr and Stéphane Minvielle Université de Nantes, CHU Nantes, CNRS, Inserm, CRCINA, F-44000 Nantes, France : stephane.minvielle@univ-nantes.fr

Running Title: Molecular signature of FDG-PET biomarkers in MM

Keywords: Multiple Myeloma; FDG-PET; CASSIOPET study; genome-wide transcriptome; RNA Sequencing.

Additional information:

Financial support: This work has been supported in part by grants from the French National Agency for Research, called "Investissements d'Avenir" IRON Labex n◦ ANR-11-LABX-0018-01; ArronaxPlusEquipex n◦ ANR-11-EQPX-0004; ISITE NExT n° ANR-16-IDEX-0007 and from SIRIC ILIAD (Imaging and Longitudinal Investigations to Ameliorate Decision-making in multiple myeloma and breast cancer) INCA-DGOS-Inserm 12558, and by Janssen Research & Development.

Conflict of interest disclosure:

- P.M.: Advisory Boards for Celgene, Janssen, Takeda, Novartis, Amgen.
- C.T. (?): Honorary and Consultancy for Celgene, Janssen, Takeda, GlaxoSmithKline, Amgen, Abbvie, and Sanofi
- Other authors: no disclosure.

Text word count: 2513/2500

Abstract word count: 242/250

Table/figure count: 4/4

Supplementary data: 5 Tables and 2 Figures

Number of references: 20/20

Abstract

Purpose: To determine molecular signature of baseline FDG-PET biomarkers in newly diagnosed multiple myeloma (MM) patients.

Experimental design: Reported prognostic biomarkers (FDG avidity, SUVmax, number of focal lesions, presence of para-medullary disease (PMD) or extra-medullary disease (EMD)) were extracted from FDG-PET imaging at baseline in a group of 139 patients from CASSIOPET, a companion study of the CASSIOPEIA cohort (ClinicalTrials.gov, NCT02541383). Transcriptomic analyses using RNA sequencing were realized on sorted bone marrow plasma cells from the same patients. Association with high-risk gene expression signature (IFM15), molecular classification, progression-free-survival (PFS), stringent clinical response (sCR) and minimal residual disease (MRD) negativity were explored.

Results: FDG-PET was positive in 79.4% of patients, with 14% and 11% of them presenting PMD and EMD respectively. Negative FDG-PET scans were associated with lower expression of hexokinase-2 (*HK2*) (Fold Change = 2.1, p_{adj}=0.02) and enriched for the LB (low-bone disease) subgroup of patients. Positive FDG-PET profiles displayed two distinct signatures with either high expression of proliferation genes, or high expression of *GLUT5* and lymphocyte antigens. PMD and IFM15 were independently associated with a lower PFS, and the presence of both biomarkers defined a group of double-positive patients at very high-risk of progression. PMD and IFM15 were neither related to MRD assessment nor to sCR.

Conclusion: Our study confirmed and extended the association between imaging biomarkers and transcriptomic programs in MM. Combined prognostic value of PMD and high-risk signature with IFM15 may help define a very high-risk group of MM.

Statement of significance

FDG-PET imaging biomarkers play a critical role in the evaluation and prognosis of multiple myeloma. Here, we confirmed and extended our understanding of the link between tumor biology and imaging biomarkers, and we showed that the combination of prognostic biomarkers from imaging and gene expression profiling may define a novel group of patients with a very high-risk of progression.

Introduction

In the past decade, there has been increasing use of positron emission tomography with 18F-fluorodeoxyglucose (FDG-PET) for the staging and therapeutic evaluation of multiple myeloma (MM) patients (1). A few studies have demonstrated the prognostic value of several biomarkers extracted from FDG-PET at baseline: the number of focal lesions (FLs), the presence or absence of extra-medullary disease (EMD), para-medullary disease (PMD), and maximum standardized glucose uptake value (SUVmax) as reviewed by Michaud-Robert *et al*. (2). Furthermore, FDG-PET is considered as negative in approximately 10–20% of MM patients (2). This pattern, associated with low expression of hexokinase-2 (*HK2*), an enzyme involved in the first step of glycolysis, is usually described as a false negative result for disease's detection but seems to carry a prognostic value (3–5). Before these FDG-PET biomarkers could be fully endorsed as risk classifiers by the haematologist community, further characterization of underlying molecular aspects is necessary. Genome-wide transcriptomic analyses through RNA-sequencing (RNA-seq) unbiasedly characterize the gene expression program of tumor cells purified from bone marrow aspirates. RNA-seq helped to understand the molecular basis of MM complexity (6,7) and to determine high-risk multiple myeloma patients with gene signatures such as GEP70, EMC-92, or IFM15 (8,9).

The purpose of this study was to identify gene expression patterns associated with prognostic FDG-PET biomarkers in newly diagnosed MM patients included in the prospective multicenter CASSIOPET study. Association with high-risk gene expression signature, molecular classification, progression-free-survival (PFS), clinical response and minimal residual disease (MRD) negativity at 100 days after autologous stem cell transplant (ASCT) were also explored.

Materials and methods

Patients

A group of 139 newly diagnosed patients from CASSIOPET (in press, (5)), a companion study of the phase 3 CASSIOPEIA trial (10), were subjected to gene expression profiling at baseline in addition to ^{18}FDG-PET/CT imaging. The aims, inclusion and exclusion criteria of CASSIOPEIA trial (ClinicalTrials.gov, NCT02541383) have previously been reported (10). The CASSIOPET study was locally approved by the institutional ethics committee (University Hospital, Nantes, France). Myeloma plasma cells were derived from bone marrow sampling collected in the Intergroupe Francophone du Myélome (IFM) and in the Dutch/Belgian Haemato -Oncology Foundation for Adults in the Netherlands (HOVON) centers. Myeloma cells were purified using nanobeads and an anti-CD138 antibody (RoboSep, Stem Cell

Technologies). The average cell purity of MM was > 99% (range 79-100) as assessed by MGG staining and morphology. Finally, all samples with available material >200ng RNA and RNA Integrity Number > 6.5 were included and sequenced.

RNA Sequencing

Libraries were prepared with NEBNext Ultra II for directional RNA sequencing kit (New England Biolabs, Ipswich, MA, ref. E7765L, E7490L, E6440S). Quality controls (QCs) were performed with High Sensitivity D1000 (Agilent, Santa Clara, CA) and NEBNext Library Quant Kit for Illumina (Ref. E7630L) on a TapeStation 2200 (Agilent, Santa Clara, CA). All libraries passed QCs and were sequenced on a NovaSeq 6000 (Illumina, San Diego, CA) with S2 flowcells at 2x100 cycles (Ref. 20012861). Finally, sequencing depth ranged from 74 to 163 million paired-reads per library. RNA-sequencing reads were aligned to the human reference genome hg38/GRCh38.p13 and genes were quantified with STAR v2.7.3 and Ensembl v99. Standardized log2 values of transcripts per million (TPM) units were used to compute high-risk and molecular classifications scores unit after removal of immunoglobulin genes (11). Threshold for high-risk classification with IFM15 (x=1.3) was defined according to Decaux et al. (9). Maximum of the weighted means was used to classify patients in the seven subgroups of the University of Arkansas for Medical Sciences (UAMS) classification (6) and GEP70 signature. DESeq2 was used to perform differential expression analysis from raw counts with plasma cell purity and site of collection (IFM or HOVON) treated as model covariates. DESeq2's variance stabilizing transformation (vst) was used for graphical representation and statistical analysis of gene expression levels.

FDG-PET/CT evaluation

FDG-PET images were acquired at baseline according to local protocol in each center and recommendations of good practice for PET imaging**.** Briefly, all patients fasted for at least 4 hours before FDG injection. Blood glucose level measured before FDG administration had to be ≤150mg/dL. Whole-body imaging was performed between 60 to 80 minutes after FDG injection (from 3 to 7 MBq/kg). FDG-PET data were centrally collected and analyzed, blinded to patient treatment and follow-up. As previously described (2,12), FDG-PET negativity, number of bone FLs, presence of EMD and PMD were reported. Bone SUVmax was determined.

MRD Assessment and clinical response

As reported in the CASSIOPEIA trial, MRD was evaluated by multiparametric flow cytometry of bone marrow aspirates at 100 days after ASCT. MRD negativity was defined as <0.001% of aberrant clonal plasma cells (10^{-5} threshold).

Clinical response was assessed according to International Myeloma Working Group (IMWG) criteria at 100 days after ASCT (13).

Statistical analysis

Quantitative biological and clinical variables were described with median and interquartile range (IQR) or mean and standard deviation. Significance of average difference between groups was assessed with the Kruskal-Wallis method and Dunn post-hoc for multiple group testing, or Wilcoxon test for 2 groups. Difference of distribution between groups was assessed with a χ^2 pearson's test (or Fisher's exact test if appropriate). Absolute χ^2 residuals greater than 2 were considered significant as post hoc. DEseq2's Wald test was used to assess the difference in gene expression between groups. For survival analysis, progression-free survival was calculated from randomization date to disease progression or death, whichever occurred first, or to the last follow-up date. Hazard ratios between groups were calculated with a Cox model. Survival curves were calculated using the Kaplan-Meier method and groups were compared using a likelihood ratio test. P-values were corrected for multiple testing with the Benjamini-Hochberg method. Adjusted p-values under 0.05 were considered significant. All calculations were performed with R 3.6.0. (R Foundation, Vienna, Austria).

Results

Demography and FDG PET results

Among the 268 patients enrolled in the CASSIOPET study, 139 patients were considered for this analysis. These patients presented with similar demographic and clinical characteristics (Age, Sex, R-ISS staging, high-risk cytogenetics, treatment arms) to those of the entire CASSIOPET population (Table S1). Our cohort included 110 patients with positive FDG-PET (79%), of which 20 (14%) and 16 (12%) had PMD or EMD respectively at baseline. Median baseline SUVmax was 3.2 (ranging from 1.5 to 12) with 35 (32%) of the 110 FDG-avid MM patients presenting a SUVmax value higher than 4.2. Sixty-four (46%) of our patients presented 3 FLs or more. Main characteristics of our cohort regarding FDG-PET imaging and gene signatures are presented in Supplementary Figure S1.

Molecular profile of patients with PET-negative scans

To understand which patients were most likely to present negative/normal FDG-PET, the expression levels of glucose transporters 1 to 5 (GLUTs) and of hexokinases 1 to 3 (HKs) were explored. *HK2* was less expressed in patients with a normal FDG-PET (Fold Change (FC) = 2.0, p=0.04, Figure 1A), however to a lesser extent than *GLUT5* (*SLC2A5*,

FC=4.2, p=7 10^{-4}), which codes for a canonical fructose receptor (14). Conversely, *GLUT3* (*SLC2A3*) was found over-expressed in negative/normal FDG-PET patients (FC=2.0, p=0.05, Figure 1A), as well as in high-risk patients assessed with the IFM15 signature (IFM15+, FC=2.1, p=0.01, Figure 1B). Expression of other HKs and GLUTs was comparable in both groups (IFM15+ and IFM15-; Figure 1B). Of note, *GLUT2* and *GLUT4* were not found expressed in this study (0 to 0.2 transcript per million on average, TPM) and were discarded from the analysis.

The UAMS molecular classification of MM in seven subgroups (CD-1, CD-2, HP, LB, MF, MS, PR) was statistically associated with FDG-PET normality (Figure 1C). In particular, an over-representation of negative FDG-PET imaging was found in the LB group compared to the reference group of HP patients. The LB group consistently showed an under-expression of *HK2* (p=9 10^{-4}) and *GLUT5* (p=1.6 10^{-5}) (Figures 1D-E).

Finally, a differential analysis of gene-expression was carried out with DEseq2, showing that 1,202 genes were deregulated between positive/abnormal and negative/normal FDG-PETs. Genes that were moderately to highly expressed (≥500 mRNA on average) and on which the condition has an important effect (Log2FC ≥ 1 in absolute value) are presented in Figure 2. Hierarchical clustering separates two groups of positive-normal FDG-PET patients with distinct signatures. Ontology analysis confirmed a strong proliferation signature (*MKI67*, *PCNA*, *TOP2A*, *STMN1*) in a proportion of FDG-PET-positive patients (Figure 2 and Table S2), while the others positive scans over-expressed lymphocyte antigens (*CD19*, *TNFSF8*/*CD30L*, *TNFSF10*/*TRAIL*) and *SLC2A5*/*GLUT5*. Conversely, negative/normal FDG-PETs showed a cellular machinery ontology (secretion, membrane, exocytosis), and regular expression of *SLC2A3*/*GLUT3*, consistent with our first result.

Molecular profile associated with FDG-PET abnormalities

Among patients with positive/abnormal FDG-PET scans, patients with high-risk GEP70 signature had more frequent PMD than GEP70 negative patients (p=0.003, Figure S2) while no association was observed with the IFM15 signature (Figure 3A). The proliferating group of the UAMS molecular classification (PR) was associated with PMD (p=0.02), while none of the LB cluster had PMD despite an abnormal FDG-PET scan (Figure 3B). Similar analyses for EMD showed significant higher proportion in IFM15+ group (p=0.02, Figure 3C) and a lack of statistical association with GEP70 (Figure S2) or molecular classification (Figure 3D). Finally, none gene expression pattern was associated to SUVmax.

Prognostic impact of FDG-PET and high-risk gene expression signatures

The median follow-up time of our cohort was 26 months (95%: 21 - 33 months), during which 26 patients (19%) progressed (disease progression or death) and 9 died (6%). Survival analyses were limited to PFS, OS was discarded due to the small number of events.

Univariate Cox analysis (Tables S3-S4) showed that imaging biomarkers and gene expression were prognostic for progression. In particular, PMD and IFM15 were strongly associated with relapse (HR_PMD=5.2, CI=[2.3-11], and HR_IFM15=4.3, CI=[1.9-9.4], respectively). The combination of PMD and IFM15 in a Cox multivariate model showed the independence of these two variables in predicting relapse (Figure 4A, HR_PMD=4.3, CI=[1.9-9.7], $p<0.001$; HR_IFM15=3.7, CI=[1.6-8.1], p=0.001). Of note, both variables remained significant in the model when accounting for R-ISS staging (Table S5). Combining both PMD and IFM15 biomarkers defined a group with a very high-risk of progression (Figure 4B; $p=4\ 10^{-5}$). Besides, PMD and IFM15 didn't correlate with deep clinical response as defined by a clinical stringent complete response, (sCR) or by a minimal residual disease (MRD) negativity at day 100 post-ASCT (Figure 4C-F).

Similarly, negative/normal FDG-PET patients, with a good prognosis, and IFM15, with a poor prognosis, seemed to complement each other in Kaplan-Meier analysis and in a Cox multivariate model (Figure 4G-H). In particular, among patients with a negative FDG-PET (n=110), IFM15 high risk signature was still associated with a shorter PFS (HR=3.9, CI=[1.8-8.8], p=0.001).

Discussion

The last decade witnessed significant progress in the development of risk classifiers derived from cytogenetics and gene expression profiling in newly diagnosed MM (8,9,15,16). Yet, intrapatient heterogeneity, inherent to this pathology, might reduce the sensitivity of these tests which are often based on a single sample from a single site which does not necessarily reflect the entire pathology (17). Thus, whole-body functional imaging such as FDG-PET has been proposed as a complementary approach for prognosis at baseline. As such, both transcriptomic and imaging approaches allow the identification of high-risk patients despite the fact that they seemed opposed in nature. The cells studied in RNA-seq come from a single, localized bone marrow aspirate, whereas FDG-PET explored whole-body spatial heterogeneity. In this context, some FDG-PET scans are depicted as negative/normal despite the clinical diagnosis established in particular by the presence of malignant plasma cells in the bone marrow aspirate. Yet, as two sides of the same coin, it seems

possible that the characteristics of these two techniques partially overlap and that the biomarkers described in FDG-TEP can find echoes in transcriptomic data beyond *HK2* underexpression shown by the first works of the Little Rock group (3).

In this study, we reported novel associations between imaging patterns and gene-expression in MM, and we extended our knowledge about the molecular profiles of negative/normal FDG-PET. Our data demonstrate that normal-negative FDG-PET scans is associated with specific expression of glucose metabolism genes and with LB molecular subgroup, while abnormal-positive FDG-PET scans are associated with markers of cell proliferation and with a distinct transcriptomic profile including the fructose transporter *GLUT5*.

The combination of PMD and IFM15 signature clearly identified a subset of patients with a higher risk of progression in our cohort. This result was independent of the patient's R-ISS grade, and therefore extended the risk classification at diagnosis. The prognostic value of PMD and/or IFM15 was independent of an undetectable MRD or a stringent complete response. Interestingly, the only R-ISS stage 1 patient who was double positive for PMD and IFM15 progressed in four months and died within two years. Further studies could extend these observations to overall survival, and compare this new biomarker to other very-high-risk groups such as the "Double-Hit" (18).

As for the seven UAMS molecular subgroups, Usmani et al previously reported that the PR, MF, and GEP70 subgroups presented more EMD (19). These observations were not made in our study yet the PR subgroup was associated with PMD. This finding has not been raised in previous works. However, the concept of PMD, corresponding to soft tissue invasion with contiguous bone involvement, is relatively recent. The CassioPET prospective study was the first to examine and report the prognostic value of this particular imaging biomarker (5). It is plausible that these 2 entities were mixed in previous works, explaining these discordant results.

Concerning patients with negative/normal FDG-PET scans at diagnosis, they were more likely to belong to the LB subgroup of the UAMS classification, a consistent result since this cluster is characterized by a low number of FLs detected on MRI, and both groups have a good clinical prognosis. This observation had not been made in previous studies.

We also confirmed the under-expression of *HK2* in this subgroup, and showed that *GLUT3* and especially *GLUT5* were deregulated to a greater extent than *HK2* between negative/normal and positive/abnormal FDG-PET scans. More generally, when we extended our analysis to all genes, two transcriptomic signatures stood out for MM patients with positive FDG-PET: the first involved proliferation genes (*MKI67*, *PCNA*, *TOP2A*, *STMN1*) and proliferation groups (PR and MS). The second involved *GLUT5* and lymphocyte antigens such as *CD19*, *CD30L* and *TRAIL*, suggesting that a

particular gene expression program is associated with glucose avidity independently of proliferation. This observation would need to be validated at the protein level.

Similarly, 2 observations were made that require further investigations. Firstly, strong expression of *GLUT5*/*SLC2A5* was associated with positive FDG-PET. This result was unexpected since *GLUT5* does not transport glucose but fructose (14). High expression of *GLUT5* in FDG-avid tissues has been reported in the literature as a "discrepancy" in breast cancer cells expressing low levels of *GLUT1* (20). Finally, although previously described (2), the prognostic value of SUVmax using a threshold of 4.2 did not appear significant in our work in multivariate analysis.

Conclusion

This study enabled a better characterization of molecular signature of FDG-PET biomarkers. Moreover, combined prognostic value of PMD and high-risk signature with IFM15 may help define a very high-risk group of MM. This work demonstrated, once again, the added prognostic value of integrating FDG-PET in the management of MM patients.

Acknowledgments

The authors thank Elise Douillard, Magali Devic, and Nathalie Roi for their excellent technical expertise and the Biogenouest sequencing platform GenoBird in Nantes, France for the Illumina sequencing.

References

1. Cavo M, Terpos E, Nanni C, Moreau P, Lentzsch S, Zweegman S, et al. Role of 18F-FDG PET/CT in the diagnosis and management of multiple myeloma and other plasma cell disorders: a consensus statement by the International Myeloma Working Group. Lancet Oncol. 2017;18:e206–17.

2. Michaud-Robert A-V, Jamet B, Bailly C, Carlier T, Moreau P, Touzeau C, et al. FDG-PET/CT, a Promising Exam for Detecting High-Risk Myeloma Patients? Cancers. 2020;12:1384.

3. Rasche L, Angtuaco E, McDonald JE, Buros A, Stein C, Pawlyn C, et al. Low expression of hexokinase-2 is associated with false-negative FDG–positron emission tomography in multiple myeloma. Blood. 2017;130:30–4.

4. Abe Y, Ikeda S, Kitadate A, Narita K, Kobayashi H, Miura D, et al. Low hexokinase-2 expression-associated

false-negative 18F-FDG PET/CT as a potential prognostic predictor in patients with multiple myeloma. Eur J Nucl Med Mol Imaging. 2019;46:1345–50.

5. Moreau P, Zweegman S, Perrot A, Hulin C, Caillot D, Facon T, et al. Evaluation of the Prognostic Value of Positron Emission Tomography-Computed Tomography (PET-CT) at Diagnosis and Follow-up in Transplant-Eligible Newly Diagnosed Multiple Myeloma (TE NDMM) Patients Treated in the Phase 3 Cassiopeia Study: Results of the Cassiopet Companion Study [Internet]. 2019 [cited 2020 Oct 8]. Available from: https://ashpublications.org/blood/article/134/Supplement_1/692/426402/Evaluation-of-the-Prognostic-Value-of-Positron

6. Zhan F, Huang Y, Colla S, Stewart JP, Hanamura I, Gupta S, et al. The molecular classification of multiple myeloma. Blood. 2006;108:2020–8.

7. Broyl A, Hose D, Lokhorst H, de Knegt Y, Peeters J, Jauch A, et al. Gene expression profiling for molecular classification of multiple myeloma in newly diagnosed patients. Blood. 2010;116:2543–53.

8. Shaughnessy JD, Zhan F, Burington BE, Huang Y, Colla S, Hanamura I, et al. A validated gene expression model of high-risk multiple myeloma is defined by deregulated expression of genes mapping to chromosome 1. Blood. 2007;109:2276–84.

9. Decaux O, Lodé L, Magrangeas F, Charbonnel C, Gouraud W, Jézéquel P, et al. Prediction of Survival in Multiple Myeloma Based on Gene Expression Profiles Reveals Cell Cycle and Chromosomal Instability Signatures in High-Risk Patients and Hyperdiploid Signatures in Low-Risk Patients: A Study of the Intergroupe Francophone du Myélome. J Clin Oncol. 2008;26:4798–805.

10. Moreau P, Attal M, Hulin C, Arnulf B, Belhadj K, Benboubker L, et al. Bortezomib, thalidomide, and dexamethasone with or without daratumumab before and after autologous stem-cell transplantation for newly diagnosed multiple myeloma (CASSIOPEIA): a randomised, open-label, phase 3 study. The Lancet. 2019;394:29–38.

11. Barwick BG, Neri P, Bahlis NJ, Nooka AK, Dhodapkar MV, Jaye DL, et al. Multiple myeloma immunoglobulin lambda translocations portend poor prognosis. Nat Commun. 2019;10:1–13.

12. Michaud-Robert A-V, Zamagni E, Carlier T, Bailly C, Jamet B, Touzeau C, et al. Glucose Metabolism Quantified by SUVmax on Baseline FDG-PET/CT Predicts Survival in Newly Diagnosed Multiple Myeloma Patients: Combined Harmonized Analysis of Two Prospective Phase III Trials. Cancers. 2020;12:2532.

13. Kumar SK, Paiva B, Anderson KC, Durie B, Landgren O, Moreau P, et al. International Myeloma Working

Group consensus criteria for response and minimal residual disease assessment in multiple myeloma. Lancet Oncol. 2016;17:e328–46.

14. Nomura N, Verdon G, Kang HJ, Shimamura T, Nomura Y, Sonoda Y, et al. Structure and mechanism of the mammalian fructose transporter GLUT5. Nature. 2015;526:397–401.

15. Avet-Loiseau H, Li C, Magrangeas F, Gouraud W, Charbonnel C, Harousseau J-L, et al. Prognostic Significance of Copy-Number Alterations in Multiple Myeloma. J Clin Oncol. 2009;27:4585–90.

16. Avet-Loiseau H, Attal M, Moreau P, Charbonnel C, Garban F, Hulin C, et al. Genetic abnormalities and survival in multiple myeloma: the experience of the Intergroupe Francophone du Myélome. Blood. 2007;109:3489–95.

17. Rasche L, Chavan SS, Stephens OW, Patel PH, Tytarenko R, Ashby C, et al. Spatial genomic heterogeneity in multiple myeloma revealed by multi-region sequencing. Nat Commun. 2017;8:268.

18. Walker BA, Mavrommatis K, Wardell CP, Ashby TC, Bauer M, Davies F, et al. A high-risk, Double-Hit, group of newly diagnosed myeloma identified by genomic analysis. Leukemia. 2019;33:159–70.

19. Usmani SZ, Heuck C, Mitchell A, Szymonifka J, Nair B, Hoering A, et al. Extramedullary disease portends poor prognosis in multiple myeloma and is over-represented in high-risk disease even in the era of novel agents. Haematologica. 2012;97:1761–7.

20. Hamann I, Krys D, Glubrecht D, Bouvet V, Marshall A, Vos L, et al. Expression and function of hexose transporters GLUT1, GLUT2, and GLUT5 in breast cancer—effects of hypoxia. FASEB J. 2018;32:5104–18.

Figure legends

Figure 1

Molecular profile of FDG-PET negativity in the CASSIOPET trial. A. Expression of glucose transporters (GLUTs) and hexokinases (HKs) in abnormal-positive (orange) versus normal-negative (green) FDG-PET scans from the CASSIOPET cohort. **B**. Expression of GLUTs and HKs in standard risk (blue) versus high-risk (red) gene expression signature IFM15. **C**. Distribution of normal FDG-PET across multiple myeloma molecular classes as defined by the UAMS. **D-E**. Expression of HK2 (D) and GLUT5 (E) in multiple myeloma molecular classes. N=139 patients. *: $p<0.05$; **: $p<0.01$; ***:$p<0.001$; ****: $p<0.0001$. Gene expression levels are given in vst normalized counts (see Methods).

Figure 2

Gene expression profiling of abnormal FDG-PET scans. Heatmap representation of the standardized gene expression level of the most differentially expressed genes between the two conditions (normal or abnormal FDG-TEP) with DESeq2 R package. *SLC2A3* (respectively *SLC2A5*) encodes GLUT3 (resp. GLUT5).

Figure 3

Molecular profiles of FDG-PET para- and extra-medullary disease. A-B. Distribution of patients presenting para-medullary disease at baseline in IFM15 high and standard risk expression signature (A) and across myeloma molecular classes (B). **C-D.** Distribution of patients presenting extra-medullary disease at baseline in IFM15 high and standard risk expression signature (C) and across myeloma molecular classes (D). n.s.: not significant ($p>0.05$).

Figure 4

Prognostic value of imaging and gene expression profiles in the CASSIOPET cohort. A. Multivariate cox modeling of progression-free survival (PFS) by the presence of para-medullary disease (PMD) and an IFM15 high-risk gene expression signature (IFM15+). **B.** Kaplan-Meier curves representing PFS of CASSIOPET patients separated by IFM15 and PMD status. **C-D.** Distribution of MRD status at day 100 post-ASCT by baseline IFM15 status (C) and baseline PMD status (D). For MRD only, data is available for N=120 patients. **E-F.** Distribution of stringent complete response (sCR) at day 100 post-ASCT by baseline IFM15 status (E) and presence of PMD at baseline (F). **G**. Kaplan-Meier curves depicting progression-free survival (PFS) of patients with positive FDG-PET only (N=110/139) and according to their IFM15 risk status. **H**. Multivariate cox modeling of PFS using PET (normal/abnormal) and IFM15 (Yes=high-risk, No=standard risk) binary variables.

Figure 1

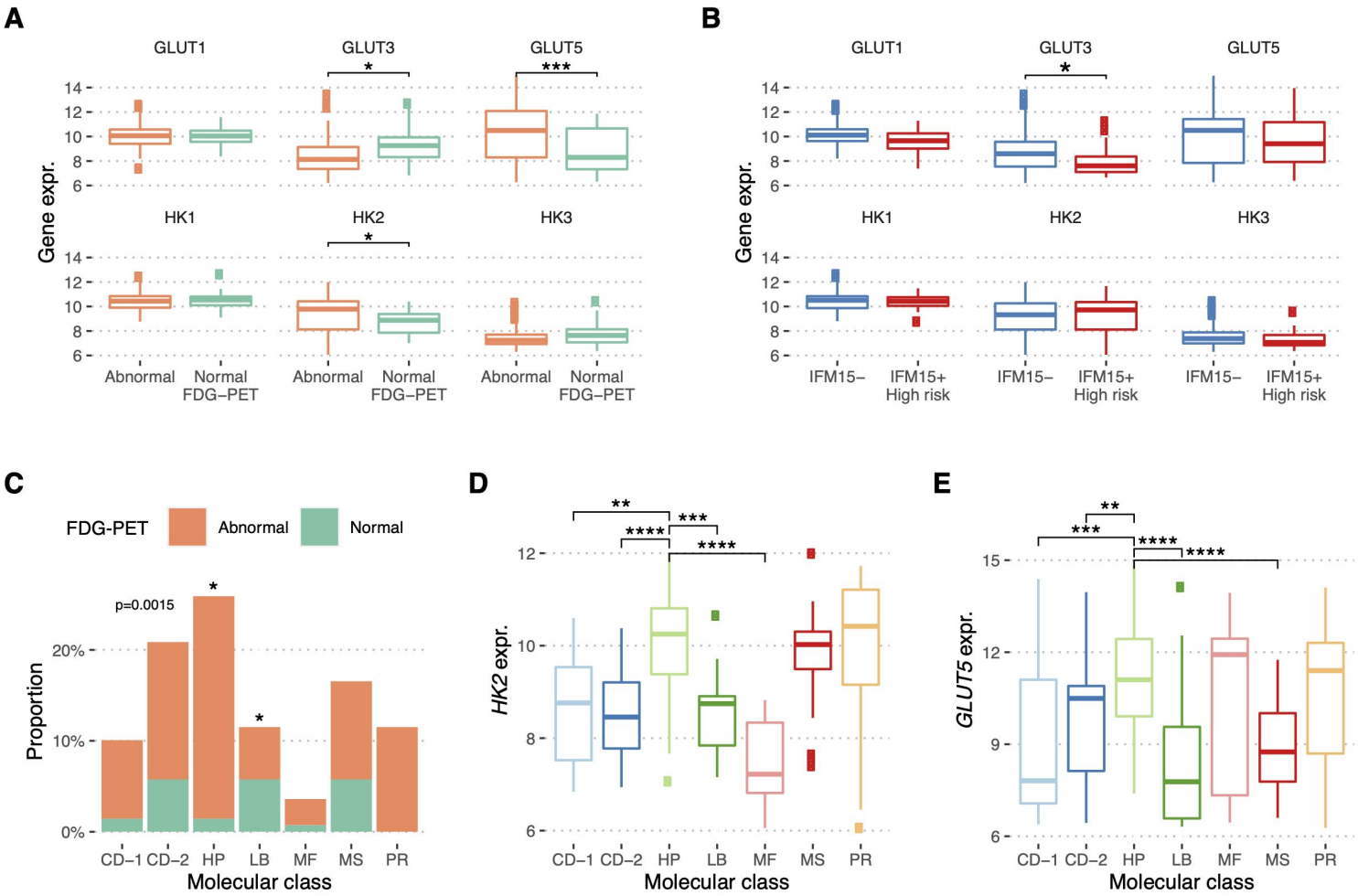
A
GLUT1
GLUT3
GLUT5
HK1
HK2
HK3
Gene expr.
Abnormal
Normal FDG−PET
B
IFM15−
IFM15+ High risk
C
FDG-PET
Abnormal
Normal
p=0.0015
Proportion
20%
10%
0%
CD−1 CD−2 HP LB MF MS PR
Molecular class
D
HK2 expr.
E
GLUT5 expr.

Figure 2

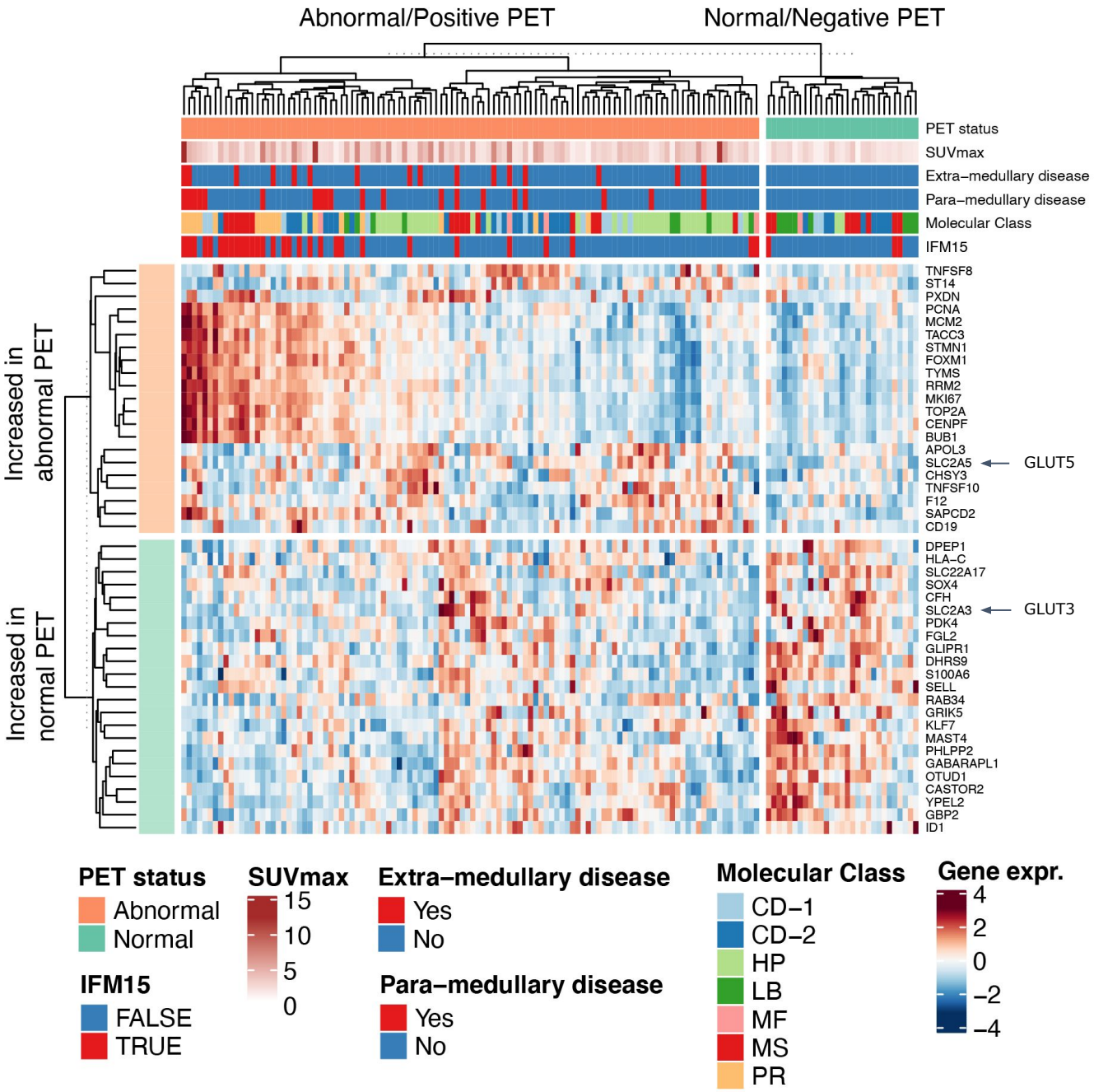
Abnormal/Positive PET
Normal/Negative PET
PET status
SUVmax
Extra−medullary disease
Para−medullary disease
Molecular Class
IFM15
Increased in abnormal PET
Increased in normal PET
TNFSF8
ST14
PXDN
PCNA
MCM2
TACC3
STMN1
FOXM1
TYMS
RRM2
MKI67
TOP2A
CENPF
BUB1
APOL3
SLC2A5
GLUT5
CHSY3
TNFSF10
F12
SAPCD2
CD19
DPEP1
HLA−C
SLC22A17
SOX4
CFH
SLC2A3
GLUT3
PDK4
FGL2
GLIPR1
DHRS9
S100A6
SELL
RAB34
GRIK5
KLF7
MAST4
PHLPP2
GABARAPL1
OTUD1
CASTOR2
YPEL2
GBP2
ID1
PET status
Abnormal
Normal
IFM15
FALSE
TRUE
SUVmax
15
10
5
0
Extra−medullary disease
Yes
No
Para−medullary disease
Yes
No
Molecular Class
CD−1
CD−2
HP
LB
MF
MS
PR
Gene expr.
4
2
0
−2
−4

Figure 3

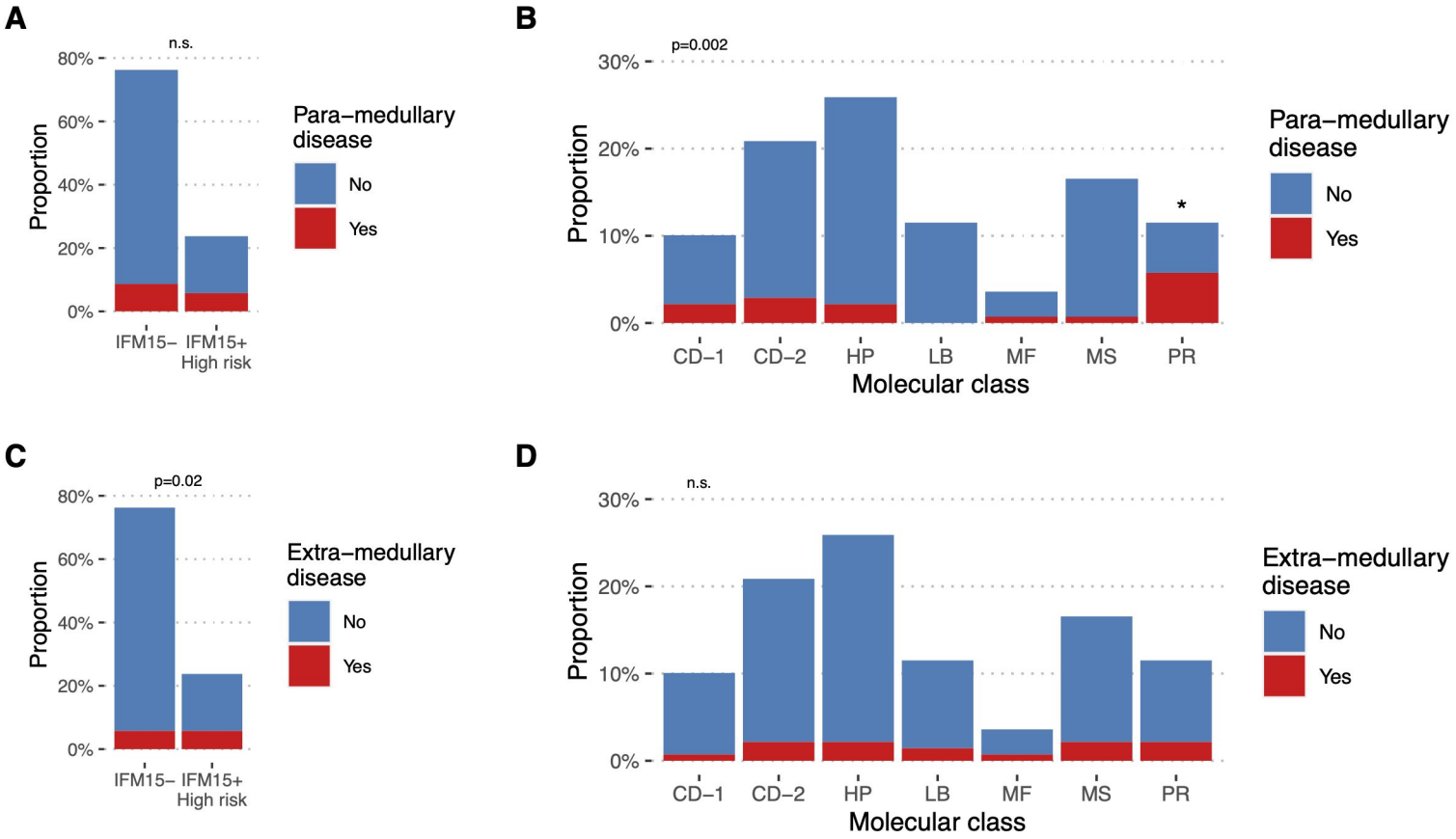
A
n.s.
80%
60%
40%
20%
0%
Proportion
IFM15−
IFM15+
High risk
Para−medullary disease
No
Yes
B
p=0.002
30%
20%
10%
0%
Proportion
CD−1
CD−2
HP
LB
MF
MS
PR
*
Molecular class
Para−medullary disease
No
Yes
C
p=0.02
80%
60%
40%
20%
0%
Proportion
IFM15−
IFM15+
High risk
Extra−medullary disease
No
Yes
D
n.s.
30%
20%
10%
0%
Proportion
CD−1
CD−2
HP
LB
MF
MS
PR
Molecular class
Extra−medullary disease
No
Yes

Figure 4

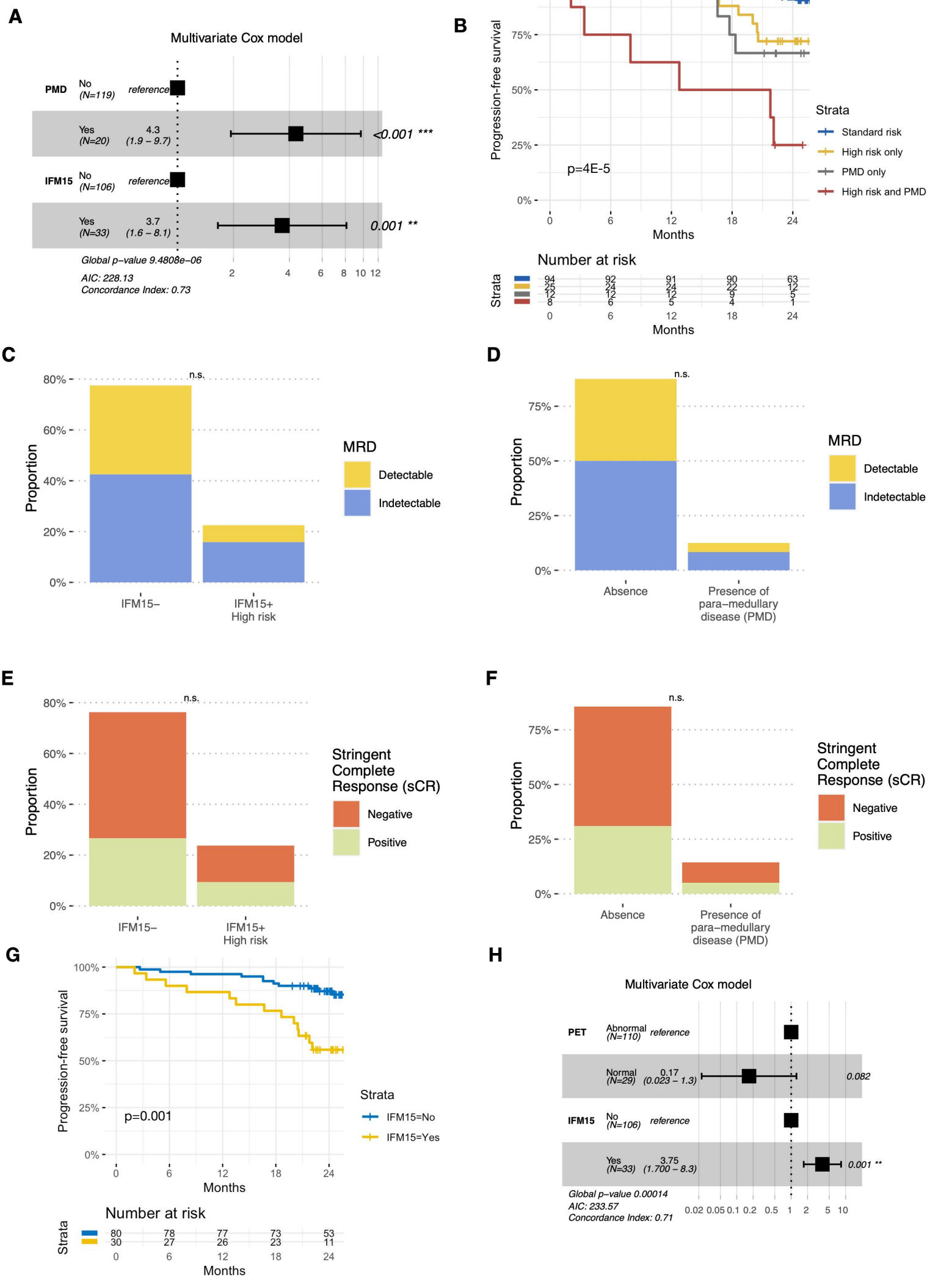
A
Multivariate Cox model
PMD
No (N=119) reference
Yes (N=20) 4.3 (1.9 – 9.7) <0.001 ***
IFM15
No (N=106) reference
Yes (N=33) 3.7 (1.6 – 8.1) 0.001 **
Global p–value 9.4808e–06
AIC: 228.13
Concordance Index: 0.73
2 4 6 8 10 12
B
Progression-free survival
100%
75%
50%
25%
0%
p=4E-5
0 6 12 18 24
Months
Strata
Standard risk
High risk only
PMD only
High risk and PMD
Number at risk
Strata
94 92 91 90 63
25 24 24 22 12
12 12 12 9 5
8 6 5 4 1
0 6 12 18 24
Months
C
Proportion
80%
60%
40%
20%
0%
n.s.
IFM15–
IFM15+ High risk
MRD
Detectable
Indetectable
D
Proportion
75%
50%
25%
0%
n.s.
Absence
Presence of para–medullary disease (PMD)
MRD
Detectable
Indetectable
E
Proportion
80%
60%
40%
20%
0%
n.s.
IFM15–
IFM15+ High risk
Stringent Complete Response (sCR)
Negative
Positive
F
Proportion
75%
50%
25%
0%
n.s.
Absence
Presence of para–medullary disease (PMD)
Stringent Complete Response (sCR)
Negative
Positive
G
Progression-free survival
100%
75%
50%
25%
0%
p=0.001
0 6 12 18 24
Months
Strata
IFM15=No
IFM15=Yes
Number at risk
Strata
80 78 77 73 53
30 27 26 23 11
0 6 12 18 24
Months
H
Multivariate Cox model
PET
Abnormal (N=110) reference
Normal (N=29) 0.17 (0.023 – 1.3) 0.082
IFM15
No (N=106) reference
Yes (N=33) 3.75 (1.700 – 8.3) 0.001 **
Global p–value 0.00014
AIC: 233.57
Concordance Index: 0.71
0.02 0.05 0.1 0.2 0.5 1 2 5 10